Expression of Integrin-E by Mucosal Mast Cells in the Intestinal Epithelium and Its Absence in Nematode-Infected Mice Lacking the Transforming Growth Factor-1-Activating Integrin v6

American Journal of Pathology, Vol. 165, No. 1, July 2004

Expression of Integrin-α_E by Mucosal Mast Cells in the Intestinal Epithelium and Its Absence in Nematode-Infected Mice Lacking the Transforming Growth Factor-β_1-Activating Integrin $\alpha_v\beta_6$

Jeremy K. Brown, Pamela A. Knight, Alan D. Pemberton, Steven H. Wright, Judith A. Pate, Elisabeth M. Thornton, and Hugh R. P. Miller

From the Department of Veterinary Clinical Studies, Easter Bush Veterinary Centre, the University of Edinburgh, Midlothian, United Kingdom

Peak intestinal mucosal mast cell (MMC) recruitment coincides with expulsion of *Trichinella spiralis*, at a time when the majority of the MMCs are located within the epithelium in BALB/c mice. Although expression of integrin-$\alpha_E\beta_7$ by MMCs has not been formally demonstrated, it has been proposed as a potential mechanism to account for the predominantly intraepithelial location of MMCs during nematode infection. Co-expression of integrin-$\alpha_E\beta_7$ and the MMC chymase mouse mast cell protease-1, by mouse bone marrow-derived mast cells, is strictly regulated by transforming growth factor (TGF)-β_1. However, TGF-β_1 is secreted as part of a latent complex *in vivo* and subsequent extracellular modification is required to render it biologically active. We now show, for the first time, that intraepithelial MMCs express integrin-$\alpha_E\beta_7$ in *Trichinella*-infected BALB/c and S129 mice. In S129 mice that lack the gene for the integrin-β_6 subunit and, as consequence, do not express the epithelial integrin-$\alpha_v\beta_6$, integrin-α_E expression is virtually abolished and recruitment of MMCs into the intestinal epithelium is dramatically reduced despite significant overall augmentation of the MMC population. Because a major function of integrin-$\alpha_v\beta_6$ is to activate latent TGF-β_1, these findings strongly support a role for TGF-β_1 in both the recruitment and differentiation of murine MMCs during nematode infection. *(Am J Pathol 2004, 165:95–106)*

Mast cell recruitment is a common feature of helminth infections and contributes to the immunological expulsion of some, but not all, gastrointestinal nematode parasites.[1–3] Mast cells are, in addition, thought to play a significant role in allergic responses in the airways and gastrointestinal tract[4,5] and in the immune response to bacterial pathogens.[6] Although the role of mast cells in the immune expulsion of gastrointestinal nematodes remains incompletely resolved, experimental studies in rats and mice suggest that intestinal mucosal mast cell (MMC)-derived β-chymases increase intestinal epithelial permeability to macromolecules.[7,8] MMCs may, therefore, contribute to the expulsion of gastrointestinal nematodes by facilitating the pathotopic translocation of effector proteins, including immunoglobulins, into the gut lumen.[2] The predominantly intraepithelial location of mouse MMCs at the time of nematode expulsion is consistent with this hypothesis.[9]

Previous studies, by our group, have shown that expression of the MMC-specific β-chymase mouse mast cell protease-1 (mMCP-1) is strictly regulated by the multifunctional cytokine, transforming growth factor (TGF)-β_1.[10] Indeed, mouse bone marrow-derived mast cells (mBMMCs) cultured in TGF-β_1 together with interleukin (IL)-3, IL-9, and stem cell factor are highly homologous to MMCs.[10–13] In agreement with studies on T lymphocytes,[14,15] mBMMC expression of the α_E chain of integrin-$\alpha_E\beta_7$ is also TGF-β_1-dependent.[13,16] The presence of integrin-$\alpha_E\beta_7$ has been demonstrated on the surface of intraepithelial T lymphocytes *in vivo*,[15,17] but its expression by MMCs has not been previously demonstrated, although antibody-blocking studies provide indirect evidence that α_E is required for recruitment and survival of MMCs within the epithelium.[18] Given that the ligand for integrin-$\alpha_E\beta_7$, E-cadherin,[19] is expressed exclusively by epithelial cells,[20] TGF-β_1-mediated expression of integrin-$\alpha_E\beta_7$ by mMCP-1-positive mBMMCs[13] is consistent with the predominantly intraepithelial location of mMCP-1-positive MMCs during the immune rejection of gastrointestinal nematodes.[9] It therefore seems highly likely that, like intestinal epithelial T lymphocytes,[15] intraepithelial MMCs express integrin-$\alpha_E\beta_7$ through a TGF-β_1-dependent mechanism and that the interaction between integrin-$\alpha_E\beta_7$ and E-cadherin contributes to their recruitment into the intestinal epithelium during nematode infection.

Supported by the Wellcome Trust (grant no. 060312).

Accepted for publication March 12, 2004.

Address reprint requests to Jeremy K. Brown, Department of Veterinary Clinical Studies, the University of Edinburgh, Easter Bush Veterinary Centre, Midlothian, EH25 9RG, UK. E-mail: jeremy.brown2@ed.ac.uk.

TGF-β_1 is ubiquitously expressed in most tissue microenvironments but is secreted as a latent complex with latency-associated protein, derived from the N-terminal sequence of the TGF-β_1 proprotein.[21] We hypothesize that the interaction of the TGF-β_1-latency-associated protein complex with integrin-$\alpha_v\beta_6$ and the subsequent presentation of active TGF-β_1 on the surface of epithelial cells[22] is a mechanism of activating latent TGF-β_1 that is likely to be important for MMC recruitment and differentiation during gastrointestinal nematode infection. In support of this hypothesis, we have previously shown that integrin-β_6-null mutation ($\beta_6^{-/-}$) mice[23] are severely compromised in their ability to mount a MMC response during infection with *Nippostrongylus brasiliensis*.[24] However, the rat-adapted strain of *N. brasiliensis* used in these studies stimulates relatively poor MMC recruitment in the mouse (PA Knight, unpublished observation).[24] In the current study, $\beta_6^{-/-}$ and $\beta_6^{+/+}$ mice were infected with the epithelium-dwelling gastrointestinal nematode *Trichinella spiralis,* to generate a maximal MMC response. The specific aims of the current study were: 1) to formally demonstrate that MMCs express integrin-$\alpha_E\beta_7$ *in vivo*; 2) to analyze the effects of the integrin-β_6-null mutation on the TGF-β_1-dependent expression of the integrin-α_E subunit; and 3) to determine whether MMC recruitment is attenuated by the integrin-β_6-null mutation.

Materials and Methods

Unless stated otherwise, reagents were purchased from Fisher Scientific UK, Loughborough, UK.

Antibodies

Purified and fluorescein isothiocyanate (FITC)-conjugated monoclonal rat IgG_1 anti-mouse IgE (clone 23G3; SouthernBiotech, Birmingham, AL) were purchased from Cambridge BioScience, Cambridge, UK. Purified monoclonal rat IgG_{2a} anti-human integrin-α_6 (clone GoH3), control rat IgG_{2a} (clone R35-95), control rat IgG_1 (clone R3-34), and FITC-conjugated control rat IgG_1 (clone R3-34) were purchased from BD Biosciences, Cowley, UK. Purified rat IgG_{2a} anti-integrin-α_E (clone M290) and anti-integrin-β_7 hybridoma supernatant (clone M293) were provided by Dr. Peter Kilshaw (The Babraham Institute, Babraham, Cambridge, UK).[14,25] Rat anti-mMCP-1 monoclonal IgG_1 (clone RF6.1)[9] and rabbit polyclonal anti-equine tryptase immunoglobulin (Ig)[26] were purified using affinity columns (Hi-Trap NHS-activated, 1 ml; Amersham Biosciences, Little Chalfont, UK) to which 1 mg of purified protein had been coupled according to the manufacturer's instructions. Alkaline phosphatase-conjugated mouse anti-rabbit IgG (clone RG-96) and purified control rabbit IgG were purchased from Sigma-Aldrich Company, Poole, UK. Proliferating cell nuclear antigen (PCNA)-specific and negative control DAKO EPOS conjugates were purchased from DakoCytomation Ltd., Ely, UK. Fluorophore conjugated monovalent goat anti-rat IgG and anti-rabbit IgG Fab fragments (Jackson ImmunoResearch Laboratories, West Grove, PA) were purchased from Stratech Scientific, Soham, UK.

Western Blot Analysis of Mouse Bone Marrow-Derived Mast Cells with Rabbit Anti-Equine Tryptase Immunoglobulin

Bone marrow cells, prepared from 10- to 12-week-old male BALB/c mice, were cultured for 12 days *ex vivo* in the presence of recombinant human TGF-β1 (1 ng/ml; Sigma-Aldrich), recombinant mouse IL-3 (1 ng/ml; R&D Systems, Abingdon, UK), recombinant mouse IL-9 (5 ng/ml; R&D Systems), and recombinant mouse stem cell factor (50 ng/ml; PeproTech EC Ltd., London, UK).[11] The resultant mouse mBMMC cultures were extracted with 20 mmol/L of Tris-HCl, pH 7.5, containing 1 mol/L NaCl. Sodium dodecyl sulfate gels (12%) (Mini-Protean-II; Bio-Rad Laboratories, Hemel Hempstead, UK) were run containing molecular weight markers (Bio-Rad Laboratories) and mBMMC extract (equivalent of 5×10^4 cells/lane). Gels were either stained with Coomassie Brilliant Blue (Bio-Rad Laboratories), or transferred to polyvinylidene difluoride membrane (Immobilon-P; Millipore, Watford, UK) and probed with 1 μg/ml of affinity-purified rabbit anti-equine tryptase Ig[26] followed by alkaline phosphatase-conjugated mouse anti-rabbit IgG (1/20,000 dilution). Blots were developed using 5-bromo-4-chloro-3-indolyl phosphate/nitro blue tetrazolium (BCIP/NBT; Sigma-Aldrich).

Parasite Infections

All experiments involving laboratory animals were performed in accordance with the United Kingdom's Animals (Scientific Procedures) Act 1986. Integrin-β_6-null (S129 strain background; S129 $\beta_6^{-/-}$) mice[23] were originally obtained from Dr. Kairbaan Hodivala-Dilke (Cell Adhesion and Disease Laboratory, GKT School of Medicine, St. Thomas' Hospital, London, UK) and backcrossed with S129 $\beta_6^{+/+}$ controls (B&K Universal, Hull, UK). Breeding colonies of S129 $\beta_6^{-/-}$, S129 $\beta_6^{+/+}$, and BALB/c mice were maintained at the Easter Bush Veterinary Centre animal facility. Maintenance, infection, and recovery of *Trichinella spiralis* larvae were performed using standard methods.[27] Mice, 8- to 15-week-old, age- and sex-matched BALB/c (B&K Universal, Hull, UK), S129 $\beta_6^{+/+}$ (B&K), and S129 $\beta_6^{-/-}$, were infected by gavage with 250 muscle larvae in 0.2 ml of phosphate-buffered saline (PBS)/0.1% agar, freshly isolated from muscle cysts from 30- to 90-day infected BALB/c mice. Groups of mice (n = 4) were killed on days 7 and 13 (S129) or 14 (BALB/c) after infection. Adult worms were isolated from the small intestine of S129 mice using a modified Baerman's technique[1] and samples of jejunum were prepared as described below. Samples were also prepared from age-matched uninfected controls.

Isolated Jejunal Epithelial Whole Mounts

Intact sheets of jejunal epithelium that included both villi and crypts were isolated by vascular perfusion with ethylenediaminetetraacetic acid[12] from 8- to 15-week-old female BALB/c mice 14 days after infection with *T. spira-*

lis, and from age- and sex-matched uninfected controls. Isolated epithelium was allowed to settle in ice-cold PBS before transfer into −20°C absolute methanol. After 20 minutes, small volumes of methanol/epithelium suspension were air-dried onto Snow Coat X-tra-charged slides (Surgipath Europe, Peterborough, UK). Samples were rehydrated and washed in three changes of PBS before proceeding with immunocytochemistry.

Jejunal Samples for Histochemistry, Immunocytochemistry, and RNA Analysis

Age- and sex-matched S129 $\beta_6^{-/-}$ and $\beta_6^{+/+}$ mice (n = 4) were killed on days 7 and 13 after infection with *T. spiralis*, along with uninfected controls. Freshly isolated samples of jejunum were collected into RNA-Later (Ambion, Huntingdon, UK) for RNA isolation (0.5 cm) and into Carnoy's fixative for histochemistry (3 cm).[1] Samples of jejunum (3.0 cm) from mice killed on day 13 were embedded in OCT compound (BDH Laboratory Supplies, Dorset, UK) and snap-frozen in dry ice-chilled isopentane. Adult worms were isolated from the reminder of the small intestine.[1] Snap-frozen samples were also prepared from age-matched female BALB/c mice (n = 4) 14 days after infection with *T. spiralis*, and from uninfected controls. For immunocytochemistry, 10-μm cryostat sections from frozen jejunal samples were mounted on Snow Coat X-tra-charged slides, air-dried for 10 minutes, and stored at −70°C. For histochemical mast cell evaluation, Carnoy's-fixed, paraffin-embedded 4-μm microtome sections of jejunum were stained overnight in 0.5% toluidine blue in 0.5 mol/L HCl, pH 0.5, and counterstained with 1% eosin solution. Toluidine blue-stained sections prepared from S129 $\beta_6^{-/-}$ and $\beta_6^{+/+}$ mice on day 13 were also washed thoroughly with PBS and probed with anti-PCNA or control EPOS antibodies as directed by the manufacturer (DakoCytomation Ltd.). PCNA-specific labeling was visualized with 3,3′-diaminobenzidine substrate (Vector Laboratories Ltd., Peterborough, UK).

Fixation and 3,3′-Diaminobenzidine Pretreatment of Frozen Sections

Frozen sections were thawed for 10 minutes at 21°C, fixed in absolute methanol for 10 minutes at −20°C, and air-dried for a further 10 minutes under forced air. Sections were washed and rehydrated in pH 7.4 PBS containing 0.5% Tween 80 (Sigma-Aldrich). Eosinophil autofluorescence was quenched using a modified version of the procedure described by Kingston and Pearson.[28] Noneosinophil-derived endogenous peroxidase activity was quenched for 30 minutes with 1% H_2O_2 in pH 7.4 PBS containing 0.5% Tween 80. Sections were then washed with PBS and incubated for 3 minutes with 3,3′-diaminobenzidine substrate. Sections were washed thoroughly with PBS before proceeding with immunocytochemistry.

Immunocytochemistry: Standard Conditions and Reagents

Unless stated otherwise, immunocytochemical procedures were performed at 21°C under humidified conditions in a Sequenza immunostaining center (Thermo Shandon, Runcorn, UK). Antibodies and blocking sera were diluted in staining buffer (pH 7.4 PBS containing 0.5 mol/L NaCl and 0.5% Tween 80). After immunocytochemical labeling, samples were washed in PBS and mounted with no. 1.5 (0.17-mm-thick) glass coverslips (BDH Laboratory Supplies) using Mowiol (pH 8.5) mounting media (EMD Biosciences, San Diego, CA).

IgE and mMCP-1 Dual-Immunofluorescent Labeling in Isolated Jejunal Epithelium

Nonspecific immunoglobulin interactions were blocked for 1 hour with staining buffer containing 10% heat-inactivated normal mouse serum (NMS). Samples were then incubated for 30 minutes with rat IgG_1 anti-mMCP-1 or control rat IgG_1, diluted to 5 μg/ml in staining buffer and 10% NMS. After washing with PBS, slides were incubated for 30 minutes with Rhodamine Red-X (RRX)-conjugated goat anti-rat IgG Fab fragments, diluted to 4 μg/ml in staining buffer and 10% NMS. Samples were washed in PBS, blocked for 1 hour in staining buffer containing 10% heat-inactivated normal rat serum (NRtS), and then incubated for 30 minutes with FITC-conjugated rat IgG_1 anti-mouse IgE or FITC-conjugated control rat IgG_1, diluted to 5 μg/ml in staining buffer and 10% NRtS. Samples were then washed with PBS and counterstained for 10 minutes with DRAQ5 (Biostatus Limited, Shepshed, Leicestershire, UK), diluted to 5 μmol/L in PBS.

Triple-Immunofluorescent Labeling of Frozen Sections

Nonspecific immunoglobulin interactions were blocked for 1 hour with staining buffer and 10% NMS. Sections were then incubated for 1 hour with staining buffer and 10% NMS containing rat anti-mouse integrin-α_E IgG_{2a} (2 μg/ml), integrin-β_7 IgG_{2a} (1/50 dilution of hybridoma supernatant), control rat IgG_{2a} (2 μg/ml), rabbit anti-equine tryptase Ig (2 μg/ml), or control rabbit IgG (2 μg/ml). Samples were washed with PBS and incubated for 30 minutes with staining buffer and 10% NMS containing Cyanine-5 (Cy5)-conjugated goat anti-rat or goat anti-rabbit Fab fragments (2 μg/ml) as appropriate.

IgE and integrin-α_6 were labeled simultaneously using Fab fragment complexes. Samples were blocked for 1 hour with staining buffer and 10% NRtS. During this time, primary rat antibodies were incubated for 20 minutes at 21°C with fluorophore-conjugated anti-rat IgG Fab fragments in a small volume, 10 μl per 1 μg of primary antibody, of staining buffer in a microcentrifuge tube. Rat anti-mouse IgE and control IgG_1 were labeled with FITC-conjugated Fab fragments at a ratio of 5 μg of Fab fragments per μg of primary rat IgG_1. Rat anti-human

integrin-α_6 and control IgG_{2a} were labeled with RRX-conjugated Fab fragments at a ratio of 5 μg of Fab fragments per μg of primary rat IgG_{2a}. The resultant Fab fragment complexes were diluted to 4 μg/ml of primary antibody with staining buffer and 10% NRtS and incubated for 10 minutes at 21°C to block any unbound Fab fragment paratopes. Tissue sections were then incubated for 1 hour with the following combinations of Fab fragment complexes (mixed 1:1 to yield a final concentration of 2 μg/ml of each primary/control antibody): IgE-specific Fab FITC and integrin-α_6-specific Fab RRX; IgE-specific Fab FITC and isotype-matched control Fab RRX; isotype-matched control-Fab FITC and integrin-α_6-specific Fab RRX; and isotype-matched control Fab FITC and isotype-matched control Fab RRX.

Microscopy and Imaging

Bright-field images were acquired with a Sony DXC-390P 3CCD color video camera (Scion Corp., Frederick, MD) mounted on an Axiovert 100 inverted microscope (Carl Zeiss, Welwyn Garden City, UK). The RGB video signal from the camera was digitized using Scion Image (Scion Corp.) installed in a G4 Macintosh computer (Apple Computer, Cupertino, CA) fitted with a CG-7 frame grabber (Scion Corp.).

Fluorescent images were acquired using an MRC-600 confocal laser-scanning microscope (CLSM; Bio-Rad Laboratories) mounted on an Axiovert 100 inverted microscope equipped with Plan-Apochromat objective lenses (Carl Zeiss). Fluorophores were excited and imaged sequentially using the 488-nm (FITC), 568-nm (RRX), and 647-nm (DRAQ5 and Cy5) lines from a 15 mW Kr/Ar laser (Bio-Rad Laboratories).

Toluidine blue-based mast cell counts were determined from 20 jejunal villus-crypt units (VCU) per mouse. The proportion of mast cells expressing PCNA in samples from $\beta_6^{-/-}$ and $\beta_6^{+/+}$ S129 mice on day 13 after infection was determined by evaluation of 200 toluidine blue-positive mast cells per mouse. Manual cell counting and stereology measurements (Cavalieri method)[29] were performed on images of fluorescently labeled samples using custom software developed for Object-Image.[30] Object-Image is a public domain software package, based on NIH Image,[31] developed by Norbert Vischer (The University of Amsterdam, Amsterdam, The Netherlands) and is available via the Internet at *http://simon.bio.uva.nl/object-image.html*. Images were prepared for publication using Object-Image and Photoshop [Adobe Systems (UK), Uxbridge, UK].

Detection of Integrin Transcripts by Semiquantitative Reverse Transcriptase-Polymerase Chain Reaction (RT-PCR)

Total RNA was extracted from RNA-Later (Ambion)-fixed jejunal samples using Tri-Reagent (Sigma-Aldrich) and contaminating DNA removed using DNA-free DNase (Ambion).[1] One mg of RNA was reverse-transcribed using 2.5 mmol/L $(dT)_{15}$. A one-twentieth volume was amplified by PCR using gene-specific primers for α_E [AED (sense), CCCTTACTCTCCTTAGGACGATCAA; AEF (anti-sense), TATCAGTCATCAAAACGCATG] that give a RT-PCR product of 197 bp, and β_7 [B7D (sense), GCTCTCTGTGGAAATCTACGA, B7F (anti-sense), TCACTCTGAAAAATCTCAGCG) that give a RT-PCR product of 278 bp, or for the housekeeping gene GAPDH,[1] with equivalent quantities of nonreverse-transcribed RNA as negative controls. Reaction conditions were optimized to ensure the number of thermocycles used coincided with the amplification phase of the PCR. Amplifications were performed for 40 seconds at 94°C, 40 seconds at 55°C, and 120 seconds at 72°C for 34 thermocycles for α_E and β_7, and for 40 seconds at 94°C, 40 seconds at 60°C, and 120 seconds at 72°C for 32 thermocycles for GAPDH, in a final magnesium concentration of 1.5 mmol/L, pH 8.3. Resultant PCR products were visualized on ethidium bromide-stained 1.6% agarose gels. Images were acquired with a Kodak Digital Science Image Station 440CF (Eastman-Kodak, Rochester, NY) and analyzed using Kodak 1D Image Analysis software. PCR product identities were confirmed by Southern blotting following standard protocols and hybridized using digoxigenin-labeled gene-specific probes.[32] Internal probe sequences for the α_E/β_7 RT-PCR products were as follows; α_E; AEE (sense), AGTGCCTTTAATGAGCACGGTT; β_7; B7E (sense), ACTGGAAGCAGGACAACAAT. Primers and internal complementary probes were designed using RawPrimer (The Virtual Genome Center, *http://alces.med.umn.edu/rawprimer.html*).

Results

Surface-Bound IgE as a Phenotypic Marker of Mast Cells in the Parasitized Intestine

Intraepithelial IgE^{+ve} Cells

mMCP-1 remains highly soluble and diffuses in frozen sections resulting in poor immunocytochemical labeling (data not shown). To address this problem and to confirm previous studies that identified MMCs on the basis of IgE staining,[33,34] jejunal epithelial whole mounts from *T. spiralis*-infected (day 14) BALB/c mice ($n = 4$) were probed with mMCP-1- and IgE-specific antibodies. The distribution of mMCP-1 and IgE staining within the jejunal epithelium confirmed that cell surface-bound IgE is exclusively restricted to mMCP-1^{+ve} MMCs (Figure 1, A to D; and Table 1). Although this method of sample preparation and fixation preserved the antigenicity of IgE and mMCP-1 (Figure 1; A to D) it was incompatible with integrin immunocytochemistry (data not shown). Subsequent analysis of MMC integrin-$\alpha_E\beta_7$ expression was performed on −20°C methanol-fixed, snap-frozen sections of jejunum.

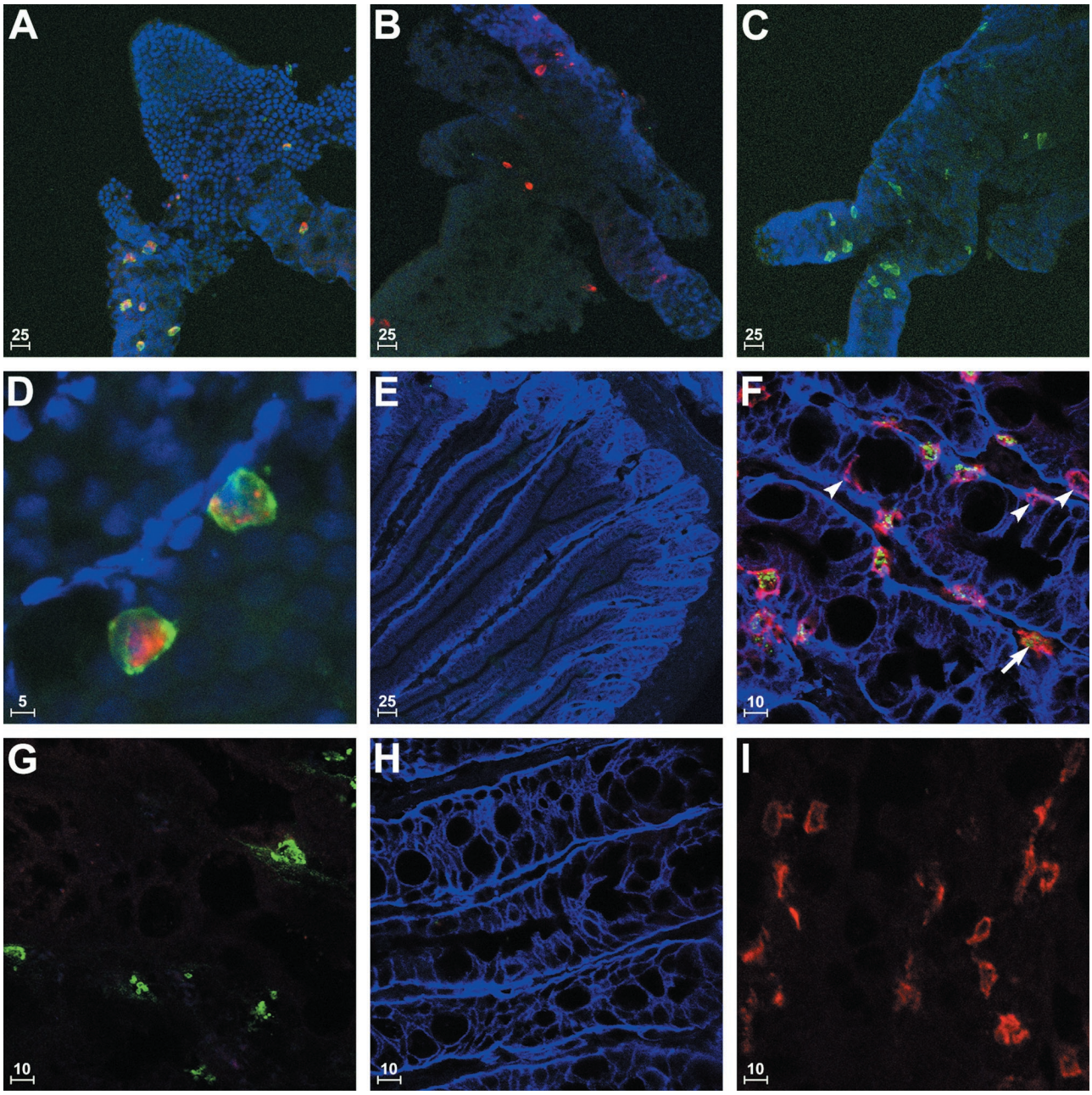

Figure 1. Immunocytochemical detection of MMCs in epithelial whole mounts and frozen sections of jejunum from *T. spiralis*-infected BALB/c mice. **A** to **D:** Whole mounts of jejunal epithelium were probed with anti-mMCP-1 (pseudo-colored red) or isotype-matched control antibodies together with anti-IgE (pseudo-colored green) or isotype-matched control antibodies and counterstained with DRAQ5 (pseudo-colored blue). IgE surface labeling was almost exclusively restricted to mast cells exhibiting strong intracellular mMCP-1 staining in samples probed with mMCP-1- and IgE-specific antibodies (**A** and **D**). Single-negative controls for IgE (**B**) and mMCP-1 (**C**) were used to confirm labeling specificity. Frozen sections of jejunum from uninfected (**E**) and *T. spiralis*-infected (**F**) BALB/c mice were probed with rabbit anti-tryptase (pseudo-colored green), anti-IgE (pseudo-colored red), and anti-integrin-α_6 antibodies (pseudo-colored blue). No IgE or tryptase-positive cells were detected in uninfected animals (**E**). Abundant IgE^{+ve} cells were detected in the samples from infected mice, the majority of which were located intraepithelially (**F**). Although significant numbers of intraepithelial IgE^{+ve} cells were tryptase-negative (**F**, **arrowheads**), most IgE^{+ve} cells detected in the lamina propria expressed tryptase (**F**, **arrow**). Staining specificity was confirmed using single-positive controls for tryptase (**G**), integrin-α_6 (**H**), and IgE (**I**), in which the two other antigen-specific antibodies were replaced with control IgG. Identical excitation and exposure settings were used to acquire images of multilabeled and control samples. Scale bar length (μm) is provided in the bottom left corner of each image.

IgE^{+ve} Cells in the Lamina Propria

IgE^{+ve} cells were enumerated in frozen sections of jejunum from *T. spiralis*-infected (day 14) BALB/c mice and uninfected controls. Although the majority of IgE^{+ve} cells within the jejunal mucosa of infected mice were located intraepithelially, substantial numbers of cells exhibiting IgE surface labeling were detected within the lamina propria (Table 2). To confirm that these cells were also mast cells, IgE staining was performed in conjunction with tryptase localization. Anti-equine tryptase[26] resulted in strong intragranular staining (Figure 1F) within >80% of IgE^{+ve} lamina propria cells and >60% of intra-

Table 1. Surface-Bound IgE as a Phenotypic Marker of Mast Cells in the Parasitized Intestinal Epithelium

Labeling	Mean (%)	Standard error of the mean (%)
IgE only	0.4	0.2
mMCP-1 only	0.9	0.3
IgE and mMCP-1	98.7	0.4

Exfoliated jejunal epithelium (−20°C methanol-fixed) from *T. spiralis*-infected BALB/c mice (day 14) was probed with anti-mMCP-1 and anti-IgE monoclonal antibodies (Figure 1; A to D). The relative frequencies of IgE single-positive (IgE only), mMCP-1 single-positive (mMCP-1 only), and IgE/mMCP-1 double-positive (IgE and mMCP-1) cells present in the epithelium were determined from a population of 500 cells/sample ($n = 4$).

epithelial IgE^{+ve} cells (Table 2). Western blot analysis of lysates from mBMMCs[11] showed that this antibody recognizes a band of ~35 kd (Figure 2) consistent with the molecular weight (MW) of glycosylated mouse tryptases (mMCP-6 and -7).[35] The relative frequencies of tryptase single-positive, IgE single-positive, and tryptase/IgE double-positive cells present in the epithelium and lamina propria were determined using integrin-α_6-specific labeling to delineate the epithelium.

IgE^{+ve} or $tryptase^{+ve}$ cells were not detected in uninfected controls (Figure 1E). Similarly, few if any, MMCs were detected in control uninfected mice by toluidine blue staining (data not shown). Nonintraepithelial $tryptase^{-ve}$ cells accounted for 1.4 ± 0.5% of the total population of IgE^{+ve} cells in the jejunal mucosa of infected mice on day 14 (Table 2). Given that only 0.4 ± 0.2% of intraepithelial IgE^{+ve} cells are mMCP-1-negative on day 14 (Table 1), IgE labeling can be used to identify mast cells within the jejunal mucosa of parasitized mice with a ≥95% degree of confidence. This is consistent with previous observations in rats and mice in which different fixation and staining techniques were used to show that IgE-bearing cells in the mucosa were mast cells and not plasma cells, macrophages, or lymphocytes.[33,34]

Table 2. Surface-Bound IgE as a Phenotypic Marker of Mast Cells in the Parasitized Intestine

Location	Labeling	Mean (%)	Standard error of the mean (%)
Epithelium	IgE only	30.6	1.9
	Tryptase only	2.3	0.6
	Dual	49.8	2.7
Lamina Propria	IgE only	1.4	0.5
	Tryptase only	1.3	0.3
	Dual	14.6	1.9

Frozen sections of jejunum (−20°C methanol-fixed) from *T. spiralis*-infected BALB/c mice (day 14) were triple-labeled with rabbit anti-equine tryptase Ig (cross-reactive with mMCP-6 and/or -7, see Figure 2), anti-IgE, and anti-integrin α_6 antibodies (Figure; 1; F to I). Using integrin α_6 staining to delineate the epithelium, the relative frequencies of IgE single-positive (IgE only), tryptase single-positive (tryptase only), and tryptase/IgE double-positive (IgE and tryptase) cells present in the epithelium and lamina propria were determined from five randomly selected 0.31-mm^2 fields of view per sample ($n = 4$).

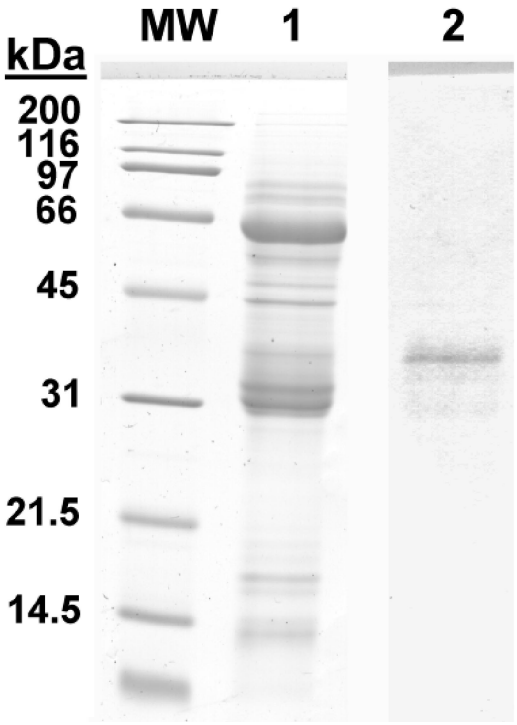

Figure 2. Detection of mouse tryptase(s) with rabbit anti-equine tryptase polyclonal antibody in Western blots of mBMMC extracts. Samples and molecular weight standards (**MW**) were run on 12% sodium dodecyl sulfate gels. Gels were stained with Coomassie Brilliant Blue (MW and **lane 1**), or transferred to Immobilon-P membrane and probed with affinity-purified rabbit anti-equine tryptase antibody (**lane 2**). Subsequent incubations with alkaline phosphatase-conjugated mouse anti-rabbit IgG and BCIP/NBT substrate resulted in the detection of a band of ~35 kd, consistent with the expected molecular weight for glycosylated murine tryptase(s), mouse mast cells protease-6, and/or protease-7.

The Integrin-α_E Subunit Is Preferentially Expressed on Intraepithelial IgE^{+ve} Cells

Frozen sections of jejunum from *T. spiralis*-infected (day 14) BALB/c mice and uninfected controls ($n = 4$) were labeled with integrin-α_E- or -β_7-specific antibodies together with IgE- and integrin-α_6-specific Fab fragment complexes. Using integrin-α_6 to differentiate the epithelium and lamina propria, the relative frequencies of IgE single-positive cells and IgE/integrin double-positive cells present in each location were determined and stereology was used to calculate IgE^{+ve} cells mm^{-2} (Figure 3). Although integrin-α_E- and -β_7-positive cells were present, IgE^{+ve} cells were not found in sections from uninfected mice (data not shown). Infection with *T. spiralis* was associated with a substantial IgE^{+ve} cell recruitment, with the majority (79.1 ± 1.5%) of IgE^{+ve} cells located within the epithelium (Figure 3A). Nearly all of the IgE^{+ve} cells present within the jejunal mucosa expressed integrin-β_7, regardless of their location (Figure 3B). Integrin-α_E was expressed by 17.1 ± 1.3% of lamina propria IgE^{+ve} cells and was detected on a significantly ($P < 0.01$; unpaired Student's *t*-test with Welch correction) higher proportion (54.5 ± 2.9%) of intraepithelial IgE^{+ve} cells (Figure 3B).

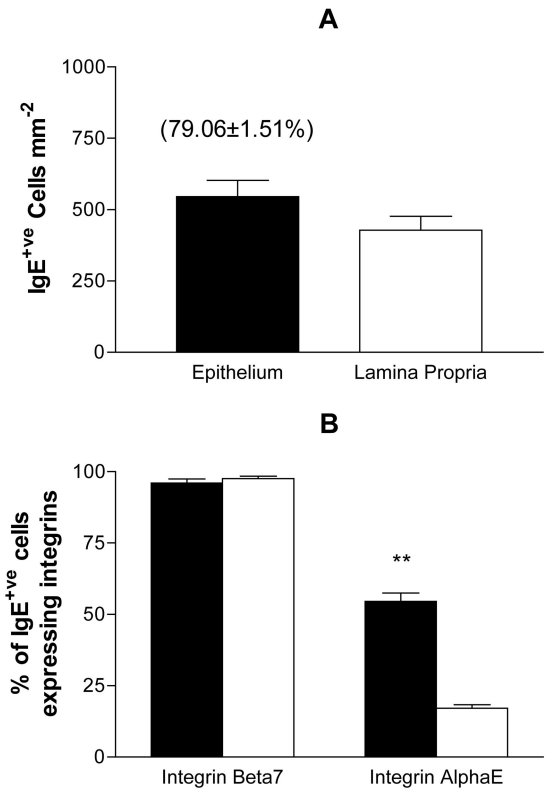

Figure 3. IgE^{+ve} cells in the jejunal mucosa of *T. spiralis*-infected mice express integrin-$\alpha_E\beta_7$. Frozen sections of jejunum from infected BALB/c mice were triple-labeled with anti-integrin-α_E or anti-integrin-β_7 together with anti-IgE and anti-integrin-α_6 (see Figure 4). Using integrin-α_6 staining to differentiate the epithelium (**filled bars**) and lamina propria (**open bars**), IgE^{+ve} cells mm^{-2} (**A**) and the relative frequencies of IgE^{+ve} cells expressing integrin-α_E or integrin-β_7 (**B**) were determined for each location using five randomly selected 0.31-mm^2 fields of view per sample. The mean percentage of intraepithelial IgE^{+ve} cells ± 1 SEM is provided in parentheses (**A**). Data are expressed as mean values ± 1 SEM (n = 4). Differences observed between the epithelial and lamina propria compartments were significant at $P < 0.01$ (**).

Deletion of the Integrin-β_6 Gene Virtually Abolishes Integrin-α_E Expression by IgE^{+ve} Cells and Inhibits Their Recruitment into the Jejunal Epithelium

Frozen sections of jejunum (n = 3) from *T. spiralis*-infected (day 13) and uninfected control S129 $\beta_6^{+/+}$ and S129 $\beta_6^{-/-}$ mice (n = 4, frozen material from one of the S129 $\beta_6^{-/-}$ mice was damaged during processing) were labeled with integrin-α_E- or -β_7-specific antibodies together with IgE- and integrin-α_6-specific Fab fragment complexes (Figure 4). IgE^{+ve} cells were not detected in sections from uninfected mice (Figure 4, A to D). Jejunum from uninfected S129 $\beta_6^{+/+}$ mice contained abundant intraepithelial integrin-α_E^{+ve} (Figure 4C) and integrin-β_7^{+ve} cells (Figure 4A). Integrin-β_7^{+ve} cells were also present in large numbers in the jejunum of uninfected S129 $\beta_6^{-/-}$ mice but were predominantly restricted to the lamina propria (Figure 4B). Integrin-α_E^{+ve} cells were extremely rare in samples from uninfected S129 $\beta_6^{-/-}$ mice and expressed substantially lower levels of integrin-α_E (Figure 4D).

Infection with *T. spiralis* was associated with IgE^{+ve} cell recruitment in both S129 $\beta_6^{+/+}$ and S129 $\beta_6^{-/-}$ mice (Figure 4E and Figure 5H). However, the frequency and distribution of IgE^{+ve} cells differed markedly in the two genotypes (Figure 5A). As observed in BALB/c mice (Figure 3A), IgE^{+ve} cell counts per unit area did not differ significantly between the epithelium and lamina propria in S129 $\beta_6^{+/+}$ mice (Figure 5A), despite the fact that the majority of the IgE^{+ve} cell population (74.1 ± 0.6%) was located intraepithelially (Figure 5B). IgE^{+ve} cell hyperplasia also occurred in S129 $\beta_6^{-/-}$ mice. However, only 18.0 ± 2.5% of IgE^{+ve} cells were located intraepithelially (Figure 5B), and there was a significant reduction ($P <$ 0.01, unpaired Student's t-test with Welch correction) in the population density of intraepithelial IgE^{+ve} cells compared to that in S129 $\beta_6^{+/+}$ mice (Figure 5A). By contrast, the population density of IgE^{+ve} cells, when compared with infected $\beta6^{+/+}$ controls, increased by more than fivefold in the lamina propria (Figure 5A) and by more than 2.5-fold in the jejunal mucosa as a whole ($P < 0.01$, unpaired Student's t-test with Welch correction).

The pattern of integrin-α_E expression in S129 $\beta_6^{+/+}$ mice was similar to that observed in BALB/c mice (Figure 3B), with 64.4 ± 8.0% of epithelial and 25.2 ± 7.2% of lamina propria IgE^{+ve} cells exhibiting strong integrin-α_E staining (Figure 5C). Integrin-α_E-positive cells were rare in sections from S129 $\beta_6^{-/-}$ mice and were typically IgE^{-ve} (Figure 4H). Only 0.2 ± 0.2% of epithelial and 1.2 ± 0.3% of lamina propria IgE^{+ve} cells showed evidence of integrin-α_E staining in S129 $\beta_6^{-/-}$ mice (Figure 5C). Virtually all IgE^{+ve} cells, regardless of their location, expressed integrin-β_7 in both S129 $\beta_6^{+/+}$ and S129 $\beta_6^{-/-}$ mice (Figure 5D).

Deletion of the Integrin-β_6 Gene Is Associated with Reduced Levels of Integrin-α_E Transcripts and Aberrant Mast Cell Distribution in the Murine Jejunum

Levels of integrin-α_E and integrin-β_7 transcripts were assessed by RT-PCR in jejunal RNA from *T. spiralis*-infected (day 13) and uninfected control S129 $\beta_6^{+/+}$ and S129 $\beta_6^{-/-}$ mice (n = 4). Although there was no evidence for a reduction in the levels of integrin-β_7 or GAPDH control transcripts in S129 $\beta_6^{-/-}$ mice, integrin-α_E transcripts appeared to be less abundant in S129 $\beta_6^{-/-}$ RNA than in wild-type samples (Figure 6A), confirming the protein expression data described earlier. Densitometry confirmed that there was a significant ($P < 0.05$, unpaired Student's t-test with Welch correction) reduction in the net intensity of integrin-α_E-specific RT-PCR products from S129 $\beta_6^{-/-}$ samples (Figure 6B).

Toluidine blue staining of Carnoy's-fixed sections (Figure 6, C and D) produced a similar pattern of staining to that observed using IgE-specific antibodies (Figure 4). Intestinal MMCs appeared to be primarily restricted to the lamina propria of S129 $\beta_6^{-/-}$ mice and were present in greater numbers (Figure 6D) than in S129 $\beta_6^{+/+}$ mice (Figure 6C). The jejunal mucosa of S129 $\beta_6^{-/-}$ mice

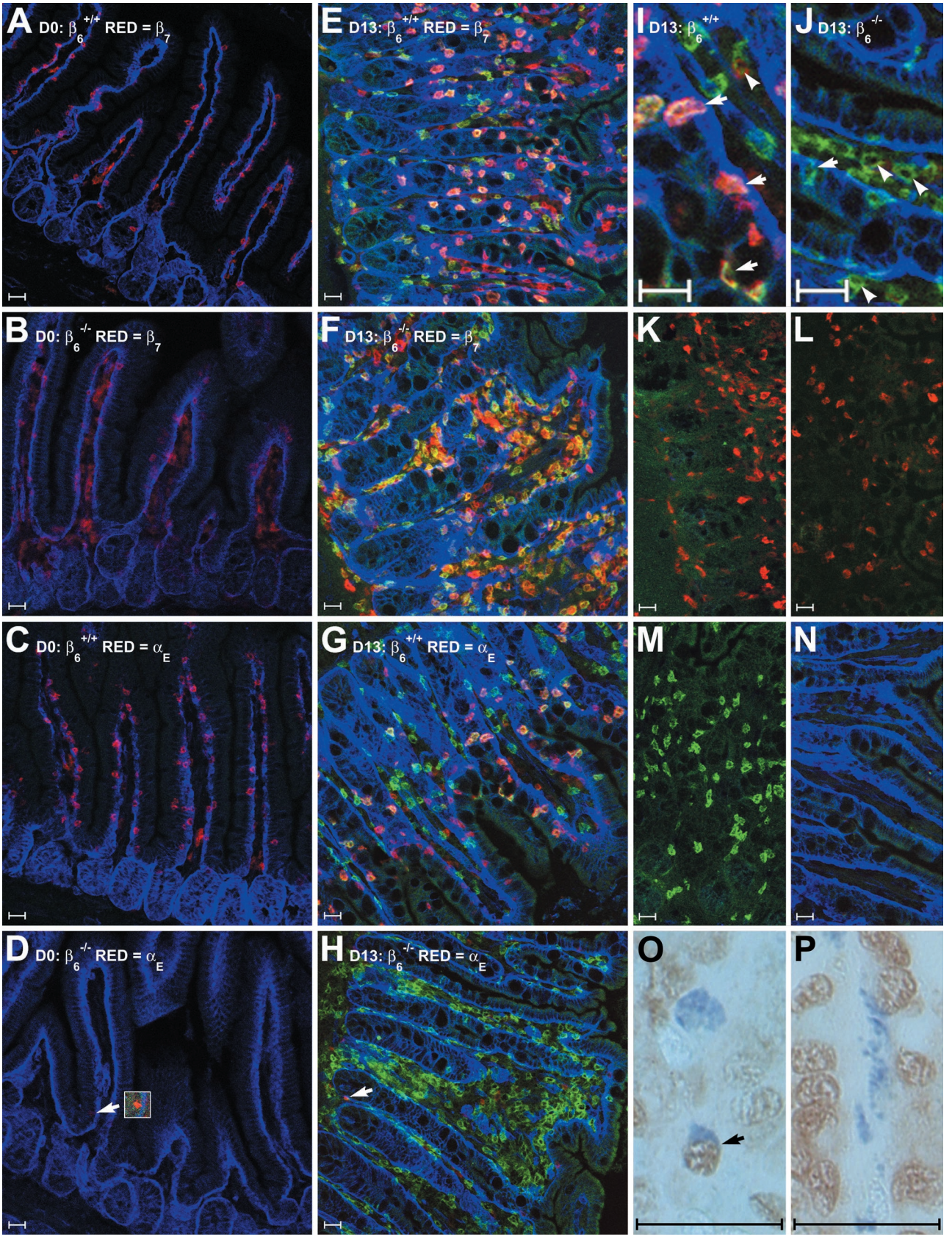
A D0: β6+/+ RED = β7
E D13: β6+/+ RED = β7
I D13: β6+/+
J D13: β6-/-
B D0: β6-/- RED = β7
F D13: β6-/- RED = β7
K
L
C D0: β6+/+ RED = αE
G D13: β6+/+ RED = αE
M
N
D D0: β6-/- RED = αE
H D13: β6-/- RED = αE
O
P

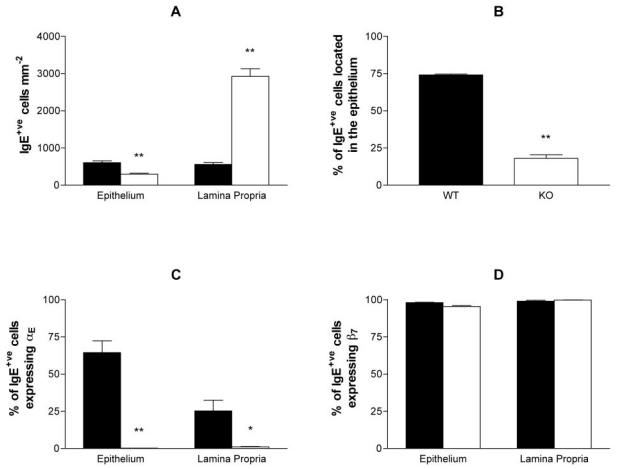

Figure 5. IgE^{+ve} cell recruitment and integrin-$\alpha_E\beta_7$ expression in the jejunal mucosa of *T. spiralis*-infected $\beta_6^{-/-}$ and $\beta_6^{+/+}$ S129 mice. Frozen sections of jejunum from infected $\beta_6^{-/-}$ (**open bars**) and $\beta_6^{+/+}$ (**filled bars**) S129 mice were triple-labeled with anti-integrin-α_E or anti-integrin-β_7 together with anti-IgE and anti-integrin-α_6 (see Figure 4). Data are presented as mean values ± 1 SEM ($n = 3$) for IgE^{+ve} cells mm^{-2} (**A**); the percentage of IgE^{+ve} cells located intraepithelially (**B**); and the relative frequencies of IgE^{+ve} cells expressing integrin-α_E (**C**) or integrin-β_7 (**D**). Differences observed between $\beta_6^{-/-}$ and $\beta_6^{+/+}$ S129 mice were significant at $P < 0.05$ (*) and $P < 0.01$ (**).

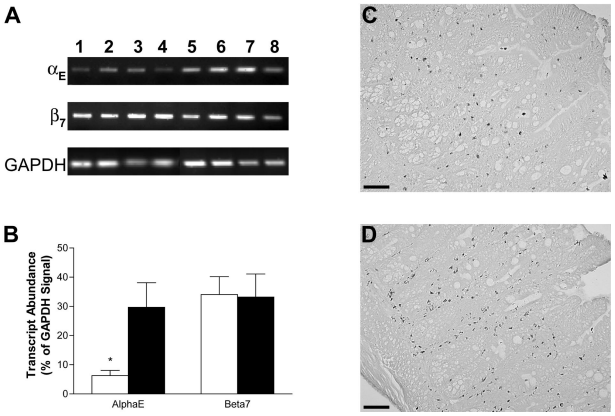

Figure 6. RT-PCR analysis of integrin-α_E and -β_7 transcript abundance and toluidine blue analysis of MMC distribution in the jejunal mucosa of *T. spiralis*-infected $\beta_6^{+/+}$ and $\beta_6^{-/-}$ S129 mice. **A:** RT-PCR products for integrin-α_E, integrin-β_7, and the housekeeping gene GAPDH from reverse-transcribed total jejunal RNA from infected $\beta_6^{-/-}$ (**lanes 1** to **4**) and $\beta_6^{+/+}$ (**lanes 5** to **8**) mice. **B:** RT-PCR product signal intensity expressed as a percentage of GAPDH signal intensity. Differences in PCR product abundance between $\beta_6^{+/+}$ and $\beta_6^{-/-}$ S129 mice were significant at $P < 0.05$ (*). Mast cells were identified using toluidine blue staining (pH 0.5) in Carnoy's-fixed/paraffin-embedded sections from $\beta_6^{+/+}$ (**C**) and $\beta_6^{-/-}$ (**D**) S129 mice. Note that mast cells are present in greater numbers in $\beta_6^{-/-}$ mice but are predominantly restricted to the lamina propria. Scale bars, 50 μm.

contained significantly ($P < 0.01$, unpaired Student's *t*-test with Welch correction) more toluidine blue-positive mast cells on day 13 after infection but there was no evidence for any difference in mast cell numbers between S129 $\beta_6^{-/-}$ and S129 $\beta_6^{+/+}$ mice on day 7 after infection or in the uninfected controls (Table 3). PCNA-specific labeling of toluidine blue-stained sections (Figure 4, O and P) did not reveal any differences in the proportion of actively proliferating (S phase) mast cells on day 13 and was difficult to interpret at earlier time points (Table 3). Similarly, small intestinal worm burdens did not differ significantly between S129 $\beta_6^{-/-}$ and S129 $\beta_6^{+/+}$ mice at either time point. However, there was a trend toward increased worm burdens in the S129 $\beta_6^{-/-}$ mice on day 13, indicating that the integrin-β_6-null mutation may be associated with a delay in *T. spiralis* expulsion (Table 3). The toluidine blue-based mast cell counts have been repeated in an independent study in S129 $\beta_6^{-/-}$ and S129 $\beta_6^{+/+}$ mice with similar findings (data not shown).

Discussion

The results described here, show, for the first time, that a significant proportion of MMCs recruited during nematode infection express the integrin-$\alpha_E\beta_7$, that these are predominantly intraepithelial mast cells, and that their intraepithelial location is highly dependent on the integrin-$\alpha_V\beta_6$. A major difference between this and our previous study, showing a general reduction in mast cell recruitment in integrin-$\beta_6^{-/-}$ mice when compared with controls infected with rat-adapted *N. brasiliensis*,[24] is that with *T. spiralis* there was substantially enhanced recruitment of mast cells in the $\beta_6^{-/-}$ mice compared with $\beta_6^{+/+}$ controls. The intestinal nematode *T. spiralis* induces a particularly potent MMC response[36] when compared with *N. brasiliensis*[24] and this is strikingly evident from the present study.

Because we were unable to co-localize mMCP-1 and integrin-α_E in frozen sections or in whole mounts of exfoliated epithelium, we used surface-bound IgE to identify MMCs, as described by others (Figure 1 and Tables 1 and 2).[33,34] Our preliminary co-localization of mMCP-1 and IgE in exfoliated epithelium and of IgE and tryptase in lamina propria mast cells is in agreement with previous studies in which Carnoy's fixation and toluidine blue staining showing that virtually all IgE-bearing cells are mast cells in parasitized rodent intestines.[33,34] Using surface IgE as a marker, we have established that the α_E- and β_7-integrin subunits are expressed on the surface of

Figure 4. Immunofluorescent detection of integrin-α_E and -β_7 expression by IgE^{+ve} cells and PCNA-specific staining of toluidine blue-positive mast cells in the jejunal mucosa of S129 $\beta_6^{-/-}$ and $\beta_6^{+/+}$ mice. **A** to **J:** Frozen sections of jejunum were probed with monoclonal rat antibodies specific for integrin-α_6 (pseudo-colored blue), IgE (pseudo-colored green), and integrin-β_7 or -α_E (pseudo-colored red). Representative images are shown from uninfected $\beta_6^{+/+}$ (**A**) and $\beta_6^{-/-}$ (**B**) mice stained for IgE, integrin-α_6, and integrin-β_7; uninfected $\beta_6^{+/+}$ (**C**) and $\beta_6^{-/-}$ (**D**) mice stained for IgE, integrin-α_6, and integrin-α_E; *T. spiralis*-infected $\beta_6^{+/+}$ (**E**) and $\beta_6^{-/-}$ (**F**) mice stained for IgE, integrin-α_6, and integrin-β_7; and *T. spiralis*-infected $\beta_6^{+/+}$ (**G**) and $\beta_6^{-/-}$ (**H**) mice stained for IgE, integrin-α_6, and integrin-α_E. **Arrowheads** in **D** and **H** highlight occasional cells that exhibit low-level integrin-α_E immunoreactivity in sections from $\beta_6^{-/-}$ mice (**inset** in **D** has been contrast enhanced). Higher magnification images from *T. spiralis*-infected $\beta_6^{+/+}$ (**I**) and $\beta_6^{-/-}$ (**J**) mice stained for IgE, integrin-α_6, and integrin-α_E are annotated with **arrows** (intraepithelial IgE^{+ve} cells) and **arrowheads** (lamina propria IgE^{+ve} cells). Note that although large numbers of IgE^{+ve} cells are present in the mucosa of *T. spiralis*-infected $\beta_6^{-/-}$ mice, they are predominantly located in the lamina propria. Single-positive controls from $\beta_6^{+/+}$ mice for integrin-β_7 (**K**), integrin-α_E (**L**), IgE (**M**), and integrin-α_6 (**N**), in which two of the three antigen-specific antibodies were substituted with isotype-matched controls, were used to confirm staining specificity. Identical excitation and exposure settings were used to acquire images **A** to **D**. Constant excitation and exposure settings were also maintained during acquisition of images **E** to **N**. Bright-field images of toluidine blue-labeled mast cells probed with anti-PCNA antibodies from *T. spiralis*-infected $\beta_6^{+/+}$ (**O**) and $\beta_6^{-/-}$ (**P**) mice, **arrow** indicates a PCNA-positive mast cell in **O**. Scale bars, 25 μm.

Table 3. Adult Worm Burdens and Jejunal Mast Cell Numbers

Day	0	7	13
Worm burden			
$\beta_6^{+/+}$	–	62.3 ± 20.4	7.5 ± 5.2
$\beta_6^{-/-}$	–	63.3 ± 18.4	23.8 ± 7.3
Mast Cells/VCU			
$\beta_6^{+/+}$	0.3 ± 0.1	3.2 ± 0.7	6.8 ± 0.9
$\beta_6^{-/-}$	0.2 ± 0.1	4.3 ± 1.5	19.6 ± 2.1*
$PCNA^{+ve}$ Mast Cells (%)			
$\beta_6^{+/+}$	ND	ND	13.4 ± 2.2
$\beta_6^{-/-}$	ND	ND	13.3 ± 0.7

Total adult worm burdens and numbers of Toluidine Blue-positive mast cells per villus crypt unit were determined for $\beta_6^{-/-}$ and $\beta_6^{+/+}$ S129 mice on days 7 and 13 after infection with *T. spiralis*. Toluidine Blue-positive cells counts were also performed on uninfected $\beta_6^{-/-}$ and $\beta_6^{+/+}$ S129 mice (day 0). The proportion of mast cells in the S phase of cell proliferation ($PCNA^{+ve}$) was determined on day 13 after infection using PCNA immunohistochemistry and Toluidine Blue staining (Figure 4, O and P). Data are presented as mean values ± 1 SEM ($n = 4$).

*Differences observed between $\beta_6^{-/-}$ S129 mice and $\beta_6^{+/+}$ S129 controls were significant at $P < 0.01$ (unpaired Student's *t*-test with Welch correction).

MMCs *in vivo* (Figure 4). Furthermore, our data suggest that integrin-α_E expression is up-regulated on intraepithelial MMCs, compared to lamina propria MMCs (Figures 3B and 5C).

The addition of TGF-β_1 to mBMMCs induces the expression of integrin-$\alpha_E\beta_7$[16] and mMCP-1.[13] In our previous study of *N. brasiliensis*-infected $\beta_6^{-/-}$ mice,[24] we established that there was little or no mMCP-1 expression in the few MMCs that were recruited to the gut. We hypothesized that the absence of integrin-$\alpha_V\beta_6$, which is known to activate latent TGF-β_1-latency-associated protein,[22] would result in an absence of activated TGF-β_1 within the epithelium and, hence, lack of expression of mMCP-1.[24] The present results, in which there is a virtual absence of integrin-α_E-expressing MMCs and a markedly reduced level of transcription of α_E integrin, is consistent with the hypothesis that integrin-$\alpha_V\beta_6$ plays a significant role in the activation of TGF-β_1 within the epithelial compartment. In addition to integrin-$\alpha_v\beta_6$,[22] plasmin, thrombospondin-1, reactive oxygen species, matrix metalloproteinases, and various other integrin heterodimers have also been implicated in latent TGF-β activation.[37] Although the low-level expression of integrin-α_E observed in $\beta_6^{-/-}$ mice may be accounted for by one or more of these additional mechanisms, it would seem that, as is the case in lung,[22,23] integrin-$\alpha_v\beta_6$ is the predominant factor in regulating TGF-β_1 activity in the murine intestinal epithelium.

Mast cells derive from hematopoietic progenitor cells of, as yet, an incompletely defined phenotype.[38,39] Despite the massive mast cell hyperplasia induced by intestinal nematode infection, there is little evidence of mast cell progenitor (MCp) proliferation in the bone marrow or circulation, with the main site of proliferation and differentiation occurring in the jejunum.[40–42] Differentiation of MCps into mature mast cells occurs after the cells leave the blood stream and is regulated by factors in their local tissue microenvironment.[38] MCp homing to the small intestine has been shown to be dependent on expression of integrin-$\alpha_4\beta_7$.[43] Intraepithelial MCps can be readily isolated from normal intestinal epithelium and the numbers increase within 4 days of infection with *T. spiralis*.[40] The microenvironment that permits the intraepithelial expansion of MMCs includes expression of stem cell factor[44] and TGF-β_1[45] by epithelial cells and of IL-3 by intraepithelial T cells.[46] There are also reports that IL-9-expressing cells can be located within allergic airway epithelium,[47] suggesting that enteric epithelium could, similarly, support the presence of IL-9-secreting lymphocytes. These observations support the hypothesis that the conditions for MMC differentiation and proliferation exist within the jejunal epithelium.

There was striking difference between infection with *T. spiralis*, in which mast cells were very abundant in the lamina propria of $\beta_6^{-/-}$ mice, and the result of a comparable experiment with the rat-adapted strain of *N. brasiliensis*, in which very few MMCs were recruited.[24] It is, however, recognized that *T. spiralis* promotes a particularly potent MMC response[48] and the stimulus is presumably strong enough to overcome the apparent inhibitory effect on MMC recruitment of a lack of $\alpha_V\beta_6$ integrin.[24] The reason why there were more MMCs in the $\beta_6^{-/-}$ mice than in $\beta_6^{+/+}$ controls is less obvious. It could be that the slightly larger worm burden on day 13 (Table 3) provides a more potent stimulus. The preliminary analysis on day 13 using PCNA (Table 3) suggests that MMCs were proliferating at the same rate in both groups. An alternative explanation is that the failure of the cells to enter the epithelium and the probable lack of expression of mMCP-1, as described for infection with *N. brasiliensis*,[24] might result in greater retention of MMCs in $\beta_6^{-/-}$ mice. This is analogous to the augmented accumulation of MMCs in mMCP-$1^{-/-}$ mice.[1] It is possible, for example, that some intraepithelial MMCs can migrate directly into the gut lumen as a consequence of the proteolysis of tight junctions by secreted mMCP-1.[7] Alternatively, the presence of mMCP-1 in the extracellular space may promote cleavage of epithelial stem cell factor and subsequent apoptosis of MMCs[49] as they are carried up into the villus. Any loss of autoregulatory function because of the absence, or to very low levels, of mMCP-1, may disturb the rate of apoptosis and/or luminal shedding of MMCs. This is further compounded by the fact that the MMCs were unable to migrate into the epithelium.

Because the most likely defect associated with the absence of the β_6-integrin gene is a lack of activated TGF-β_1 on the basolateral membranes of enterocytes, it is possible that the reduction in intraepithelial MMCs in $\beta_6^{-/-}$ mice occurs primarily because MCps fail to express α_E, do not bind to epithelially expressed E-cadherin, and thus have a reduced ability to remain intraepithelial. If the MCps enter the lamina propria of $\beta_6^{-/-}$ mice and expand and differentiate in the relative absence of TGF-β_1, then not only would numbers in the lamina propria be increased, but the phenotype of the differentiated MMC population would also differ from that described in $\beta_6^{+/+}$ controls. As mentioned above, in our study with *N. brasiliensis*, the few MMCs that were recruited did not express mMCP-1,[24] and this is consistent with an altered MMC phenotype.

Studies using integrin-deficient mice and, more specifically, antibody neutralization of integrin-α_E in *T spiralis*-infected mice[18] suggest that integrin-$\alpha_E\beta_7$ is not only required for the retention of MCp and MMCs within the intestinal epithelium but may also be essential for the recruitment of MCps to the gut mucosa because treated mice lacked MMCs both in epithelium and lamina propria. The present results suggest that the reduced expression of integrin-α_E, as a consequence of defective processing of extracellular TGF-β_1 latency-associated protein is associated with reduced recruitment of intraepithelial MMCs but, paradoxically, results in a threefold expansion of the lamina propria MMCs.

This report is the first to demonstrate, unequivocally, that MMCs express integrin-$\alpha_E\beta_7$. Furthermore, the absence of epithelially expressed integrin-$\alpha_v\beta_6$ is associated with depletion of intraepithelial MMCs, substantial down-regulation of $\alpha_E\beta_7$ expression, and a paradoxical increase in the frequency of lamina propria MMCs.

Acknowledgments

We thank Dr. Mike Wilkinson (GlaxoSmithKline) for the donation of the Bio-Rad MRC600 confocal microscope, Dr. Peter Kilshaw (The Babraham Institute) for the provision of the anti-integrin-α_E and -β_7 monoclonal antibodies, and Dr. Kairbaan Hodivala-Dilke (St. Thomas' Hospital) for providing breeding pairs of integrin-β6-null S129 mice.

References

1. Knight PA, Wright SH, Lawrence CE, Paterson YY, Miller HRP: Delayed expulsion of the nematode Trichinella spiralis in mice lacking the mucosal mast cell-specific granule chymase, mouse mast cell protease-1. J Exp Med 2000, 192:1849–1856
2. Miller HRP: Mucosal mast cells and the allergic response against nematode parasites. Vet Immunol Immunopathol 1996, 54:331–336
3. Grencis RK, Else KJ, Huntley JF, Nishikawa SI: The in vivo role of stem cell factor (c-kit ligand) on mastocytosis and host protective immunity to the intestinal nematode Trichinella spiralis in mice. Parasite Immunol 1993, 15:55–59
4. Galli SJ: New concepts about the mast cell. N Engl J Med 1993, 328:257–265
5. Metcalfe DD, Baram D, Mekori YA: Mast cells. Physiol Rev 1997, 77:1033–1079
6. Malaviya R, Abraham SN: Mast cell modulation of immune responses to bacteria. Immunol Rev 2001, 179:16–24
7. McDermott JR, Bartram RE, Knight PA, Miller HRP, Garrod DR, Grencis RK: Mast cells disrupt epithelial barrier function during enteric nematode infection. Proc Natl Acad Sci USA 2003, 100:7761–7766
8. Scudamore CL, Jepson MA, Hirst BH, Miller HRP: The rat mucosal mast cell chymase, RMCP-II, alters epithelial cell monolayer permeability in association with altered distribution of the tight junction proteins ZO-1 and occludin. Eur J Cell Biol 1998, 75:321–330
9. Scudamore CL, McMillan L, Thornton EM, Wright SH, Newlands GF, Miller HRP: Mast cell heterogeneity in the gastrointestinal tract: variable expression of mouse mast cell protease-1 (mMCP-1) in intraepithelial mucosal mast cells in nematode-infected and normal BALB/c mice. Am J Pathol 1997, 150:1661–1672
10. Miller HRP, Wright SH, Knight PA, Thornton EM: A novel function for transforming growth factor-beta1: upregulation of the expression and the IgE-independent extracellular release of a mucosal mast cell granule-specific beta-chymase, mouse mast cell protease-1. Blood 1999, 93:3473–3486
11. Brown JK, Knight PA, Wright SH, Thornton EM, Miller HRP: Constitutive secretion of the granule chymase mouse mast cell protease-1 and the chemokine, CCL2, by mucosal mast cell homologues. Clin Exp Allergy 2003, 33:132–146
12. Rosbottom A, Scudamore CL, Von Der Mark H, Thornton EM, Wright SH, Miller HRP: TGF-beta1 regulates adhesion of mucosal mast cell homologues to laminin-1 through expression of integrin alpha7. J Immunol 2002, 169:5689–5695
13. Wright SH, Brown J, Knight PA, Thornton EM, Kilshaw PJ, Miller HRP: Transforming growth factor-beta1 mediates coexpression of the integrin subunit alphaE and the chymase mouse mast cell protease-1 during the early differentiation of bone marrow-derived mucosal mast cell homologues. Clin Exp Allergy 2002, 32:315–324
14. Kilshaw PJ, Murant SJ: Expression and regulation of beta 7(beta p) integrins on mouse lymphocytes: relevance to the mucosal immune system. Eur J Immunol 1991, 21:2591–2597
15. Suzuki R, Nakao A, Kanamaru Y, Okumura K, Ogawa H, Ra C: Localization of intestinal intraepithelial T lymphocytes involves regulation of alphaEbeta7 expression by transforming growth factor-beta. Int Immunol 2002, 14:339–345
16. Smith TJ, Ducharme LA, Shaw SK, Parker CM, Brenner MB, Kilshaw PJ, Weis JH: Murine M290 integrin expression modulated by mast cell activation. Immunity 1994, 1:393–403
17. Kilshaw PJ, Baker KC: A new antigenic determinant on intra-epithelial lymphocytes and its association with CD45. Immunology 1989, 67: 160–166
18. McDermott JR, Grencis RK, Else KJ: Leucocyte recruitment during enteric nematode infection. Immunology 2001, 103:505–510
19. Cepek KL, Shaw SK, Parker CM, Russell GJ, Morrow JS, Rimm DL, Brenner MB: Adhesion between epithelial cells and T lymphocytes mediated by E-cadherin and the alpha E beta 7 integrin. Nature 1994, 372:190–193
20. Kilshaw PJ: Alpha E beta 7. Mol Pathol 1999, 52:203–207
21. Gentry LE, Nash BW: The pro domain of pre-pro-transforming growth factor beta 1 when independently expressed is a functional binding protein for the mature growth factor. Biochemistry 1990, 29:6851–6857
22. Munger JS, Huang X, Kawakatsu H, Griffiths MJ, Dalton SL, Wu J, Pittet JF, Kaminski N, Garat C, Matthay MA, Rifkin DB, Sheppard D: The integrin alpha v beta 6 binds and activates latent TGF beta 1: a mechanism for regulating pulmonary inflammation and fibrosis. Cell 1999, 96:319–328
23. Huang XZ, Wu JF, Cass D, Erle DJ, Corry D, Young SG, Farese RV, Sheppard D: Inactivation of the integrin beta 6 subunit gene reveals a role of epithelial integrins in regulating inflammation in the lung and skin. J Cell Biol 1996, 133:921–928
24. Knight PA, Wright SH, Brown JK, Huang X, Sheppard D, Miller HRP: Enteric expression of the integrin alpha(v)beta(6) is essential for nematode-induced mucosal mast cell hyperplasia and expression of the granule chymase, mouse mast cell protease-1. Am J Pathol 2002, 161:771–779
25. Kilshaw PJ, Murant SJ: A new surface antigen on intraepithelial lymphocytes in the intestine. Eur J Immunol 1990, 20:2201–2207
26. Pemberton AD, McEuen AR, Scudamore CL: Characterisation of tryptase and a granzyme H-like chymase isolated from equine mastocytoma tissue. Vet Immunol Immunopathol 2001, 83:253–267
27. Wakelin D, Wilson MM: Transfer of immunity to Trichinella spiralis in the mouse with mesenteric lymph node cells: time of appearance of effective cells in donors and expression of immunity in recipients. Parasitology 1977, 74:215–224
28. Kingston D, Pearson JR: The use of the peroxidase reaction to obliterate staining of eosinophils by fluorescein-labelled conjugates. J Immunol Methods 1981, 44:191–198
29. Gundersen HJ, Jensen EB: The efficiency of systematic sampling in stereology and its prediction. J Microsc 1987, 147:229–263
30. Vischer NOE, Huls PG, Woldringh CL: Object-Image: an interactive image analysis program using structured point collection. Binary 1994, 6:160–166
31. Rasband WS, Bright DS: NIH Image: a public domain image processing program for the Macintosh. Microbeam Analysis 1995, 4:137–149
32. Wastling JM, Knight P, Ure J, Wright S, Thornton EM, Scudamore CL, Mason J, Smith A, Miller HRP: Histochemical and ultrastructural modification of mucosal mast cell granules in parasitized mice lacking the beta-chymase, mouse mast cell protease-1. Am J Pathol 1998, 153: 491–504

33. Mayrhofer G, Bazin H, Gowans JL: Nature of cells binding anti-IgE in rats immunized with Nippostrongylus brasiliensis: IgE synthesis in regional nodes and concentration in mucosal mast cells. Eur J Immunol 1976, 6:537–545
34. Alizadeh H, Urban JF, Katona IM, Finkelman FD: Cells containing IgE in the intestinal mucosa of mice infected with the nematode parasite Trichinella spiralis are predominantly of a mast cell lineage. J Immunol 1986, 137:2555–2560
35. Algermissen B, Laubscher JC, Bauer F, Henz BM: Purification of mast cell proteases from murine skin. Exp Dermatol 1999, 8:413–418
36. Tuohy M, Lammas DA, Wakelin D, Huntley JF, Newlands GF, Miller HRP: Functional correlations between mucosal mast cell activity and immunity to Trichinella spiralis in high and low responder mice. Parasite Immunol 1990, 12:675–685
37. Annes JP, Munger JS, Rifkin DB: Making sense of latent TGFbeta activation. J Cell Sci 2003, 116:217–224
38. Gurish MF, Boyce JA: Mast cell growth, differentiation, and death. Clin Rev Allergy Immunol 2002, 22:107–118
39. Kirshenbaum AS, Goff JP, Semere T, Foster B, Scott LM, Metcalfe DD: Demonstration that human mast cells arise from a progenitor cell population that is CD34(+), c-kit(+), and expresses aminopeptidase N (CD13). Blood 1999, 94:2333–2342
40. Dillon SB, MacDonald TT: Limit dilution analysis of mast cell precursor frequency in the gut epithelium of normal and Trichinella spiralis infected mice. Parasite Immunol 1986, 8:503–511
41. Kasugai T, Tei H, Okada M, Hirota S, Morimoto M, Yamada M, Nakama A, Arizono N, Kitamura Y: Infection with Nippostrongylus brasiliensis induces invasion of mast cell precursors from peripheral blood to small intestine. Blood 1995, 85:1334–1340
42. Tegoshi T, Okada M, Nishida M, Arizono N: Early increase of gut intraepithelial mast cell precursors following Strongyloides venezuelensis infection in mice. Parasitology 1997, 114:181–187
43. Gurish MF, Tao H, Abonia JP, Arya A, Friend DS, Parker CM, Austen KF: Intestinal mast cell progenitors require CD49dbeta7 (alpha4beta7 integrin) for tissue-specific homing. J Exp Med 2001, 194:1243–1252
44. Klimpel GR, Langley KE, Wypych J, Abrams JS, Chopra AK, Niesel DW: A role for stem cell factor (SCF): c-kit interaction(s) in the intestinal tract response to Salmonella typhimurium infection. J Exp Med 1996, 184:271–276
45. Koyama SY, Podolsky DK: Differential expression of transforming growth factors alpha and beta in rat intestinal epithelial cells. J Clin Invest 1989, 83:1768–1773
46. Barrett TA, Gajewski TF, Danielpour D, Chang EB, Beagley KW, Bluestone JA: Differential function of intestinal intraepithelial lymphocyte subsets. J Immunol 1992, 149:1124–1130
47. Toda M, Tulic MK, Levitt RC, Hamid Q: A calcium-activated chloride channel (HCLCA1) is strongly related to IL-9 expression and mucus production in bronchial epithelium of patients with asthma. J Allergy Clin Immunol 2002, 109:246–250
48. Garside P, Kennedy MW, Wakelin D, Lawrence CE: Immunopathology of intestinal helminth infection. Parasite Immunol 2000, 22: 605–612
49. Iemura A, Tsai M, Ando A, Wershil BK, Galli SJ: The c-kit ligand, stem cell factor, promotes mast cell survival by suppressing apoptosis. Am J Pathol 1994, 144:321–328